Composition of the Chandra ACIS contaminant

Herman L. Marshall[a], Allyn Tennant[b],
Catherine E. Grant[a], Adam P. Hitchcock[c], Steve O'Dell[b], and Paul P. Plucinsky[d]

[a]Center for Space Research, Massachusetts Institute of Technology, Cambridge, MA, USA 02139
[b]NASA Marshall Space Flight Center, Huntsville, AL, USA 35812
[c]Chemistry, McMaster University, Hamilton, ON, Canada L8S-9140
[d]Harvard-Smithsonian Center for Astrophysics, 60 Garden St, Cambridge, MA, USA 02138

ABSTRACT

The Advanced CCD Imaging Spectrometer (ACIS) on the Chandra X-ray Observatory is suffering a gradual loss of low energy sensitivity due to a buildup of a contaminant. High resolution spectra of bright astrophysical sources using the Chandra Low Energy Transmission Grating Spectrometer (LETGS) have been analyzed in order to determine the nature of the contaminant by measuring the absorption edges. The dominant element in the contaminant is carbon. Edges due to oxygen and fluorine are also detectable. Excluding H, we find that C, O, and F comprise >80%, 7%, and 7% of the contaminant by number, respectively. Nitrogen is less than 3% of the contaminant. We will assess various candidates for the contaminating material and investigate the growth of the layer with time. For example, the detailed structure of the C-K absorption edge provides information about the bonding structure of the compound, eliminating aromatic hydrocarbons as the contaminating material.

Keywords: Contamination, X-rays, Telescopes, Spectroscopy

1. INTRODUCTION

Plucinsky *et al.* (2003)[1] showed that the detection efficiency of the *Chandra*[2] Advanced CCD Imaging Spectrometer (ACIS)[3] declined monotonically in the first three years. The decline was particularly apparent in the strengths of the Mn and Fe L lines relative to the Mn K line from the external calibration source; this ratio dropped by 35%. The decline was attributed to the buildup of a contaminating layer on the ACIS optical blocking filter, which is colder than most components of the spacecraft interior. Plucinsky *et al.* examined data from spectroscopy using the *Chandra* Low Energy Transmission Grating Spectrometer (LETGS) used with the ACIS detector to show that the contaminant had a very strong C-K edge and a possible weak O-K edge as well. At the time, there was no detection of the N-K edge and there was only a hint of an edge at F-K.

In this paper, we construct a detailed empirical model of the absorption due to the contaminant using observations of bright continuum-dominated sources taken with the *Chandra* LETGS and ACIS. We also describe new features of this absorption model and the detection of a F-K edge. A time dependent absorption model is constructed that can be used to correct *Chandra* grating spectra for absorption. This model is compared to the results from the external calibration source. We find that there is still a component of the absorption that is unaccounted for in the new absorption model that can cause systematic errors in the effective area of up to 15%. These results rely on calibration analyses outlined by Marshall *et al.* (2003).[4]

2. EARLY RESULTS

The problem was first noticed in a Guest Observer observation (see Fig.1) of Ton S 180 taken in December 1999 (observation ID 811). This feature was subsequently detected in the calibration observation of 3C 273 (taken in January 2000; observation ID 1198). The residuals of the Ton S 180 and 3C 273 are compared in Fig.1. The similarity is quite striking and indicated that the difference was intrinsic to the instrument. The LETG/HRC-S data from 3C 273 taken immediately prior to the LETG/ACIS-S observation do not show a comparable residual, confirming that the feature is not intrinsic to the source.

Further author information: (Send correspondence to H.L.M.)
H.L.M.: E-mail: hermanm@space.mit.edu, Telephone: 1 617 253 8573

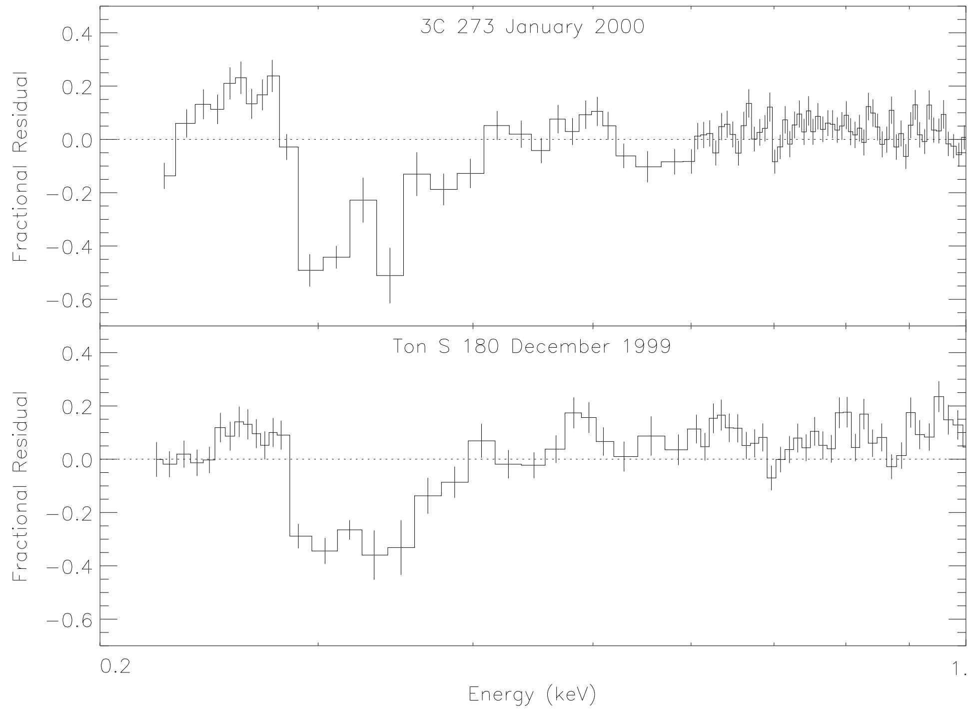

Figure 1. Comparison of two LETG/ACIS-S observations of bright continuum sources. The residuals give the fractional differences between the simple power law spectral model that was folded through the instrument response and the observed count spectra. Note the apparent edge at about 0.29 keV, which is near the K edge of carbon. The data were adaptively binned to obtain a signal to noise ratio of at lest 20 in each bin, limited to a bin width $< 5\%E$ at energy E.

In April 2000, data from a much brighter source, XTE J1118+480, were obtained. Because it was so bright at 0.28 keV, the data were not rebinned, so that the filter model could be examined in detail. Fig. 2 shows the C-K region and how a slight adjustment to the ACIS filter model in energy (0.5 eV) and in optical depth at C-K (13%) gives a good fit in the 0.283-0.287 keV region (near edge structure) but that there is a strong sharp edge above 0.287 keV. No reasonable adjustment of the filter would be able to explain the excess absorption above 0.287 keV. Fig. 3 shows that the edge is also present in the +1 order, where the C-K edge is observed on a frontside-illuminated (FI) chip, which has significantly less quantum efficiency at 0.28 keV than a backside-illuminated (BI) chip. In these early observations, there were no clear signs of other edges nor suspicion of time variability, so a simple model consisting entirely of a layer of carbon about 170 nm deep was developed to correct for the C-K edge absorption. An effective area correction was released for *Chandra* LETGS analysis in 2001 (v2.6 of the *Chandra* calibration data base).

3. REFINING THE COMPOSITION

In early 2002, there was a clear indication of a progressive drop in the ACIS low energy quantum efficiency.[1] The C-K edge absorption that had been attributed only to LETG/ACIS observations was now understood as a more general ACIS effect that was changing with time. A series of monitoring observations revealed more features as the optical depth at C-K increased. In June 2002, a 50 ks observation of PKS 2155-304 revealed an O-K edge and possible residuals at the F-K edge, as reported by Plucinsky *et al.* (2003).[1] In October, 2002, O-K and F-K edges were observed in a very long observation of Mk 421 while it was in a very bright state. A model of the absorption due to the contaminant was developed as follows.

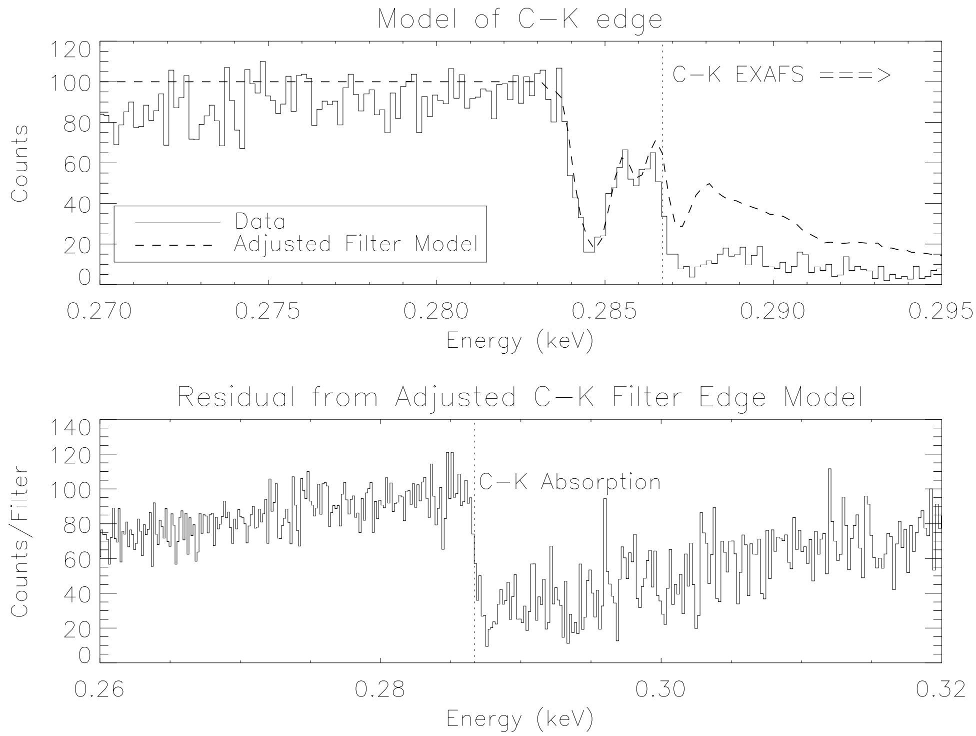

Figure 2. Modelling of the C-K edge region using the data from XTE J1118+48. The top plot shows a simple model consisting of a constant flux (at 100 counts/bin) multiplied by the carbon absorption component of the optical blocking filter (OBF) model. The optical depth of the carbon component was increased by 13% to match the data in the 0.283-0.2865 keV region. The data were then corrected by this adjusted filter model to obtain the data in the lower plot. The residual is a sharp edge recovering smoothly beyond 0.2870 keV.

3.1. Upgrading the C-K Edge Model

The observation of PKS 2155-304 in June, 2002 (observation ID 3669) was analyzed in detail to obtain a good overall spectrum, n_E, in units of ph cm^{-2} s^{-1} keV^{-1}. We used a continuum model of the form

$$N_E = \frac{K_1 E^{-\Gamma_1}}{1 + \frac{K_1}{K_2} E^{\Gamma_2 - \Gamma_1}} \tag{1}$$

where N_E is the spectral flux in the same units as n_E, K_i are the normalizations of the two components in the same units, and Γ_i are the spectral indices of the power law components. In this model, there are no spectral breaks, only smooth curvature at the point where the two power law components have equal contributions. Thus, no sharp features are added via modeling. Excluding the 0.28-1.0 keV region from the model fit gives N_E that is not affected by absorption. The ratio of the data to the model expressed as an optical depth due to absorption is computed as $-\ln(n_E/N_E)$, plotted in Fig. 4.

The data from Fig. 4 (bottom) were further rebinned in order to model the overall shape of the absorption (Fig. 5). Fig. 5 shows the new model for the C-K edge that starts with the Henke constants from the Center for X-ray Optics (CXRO*) except that the optical depth was multiplied by a damped ripple adjustment factor:

$$1 + A\exp(-x/x_d)\cos(fx) \tag{2}$$

*See `http://www.cxro.lbl.gov/`.

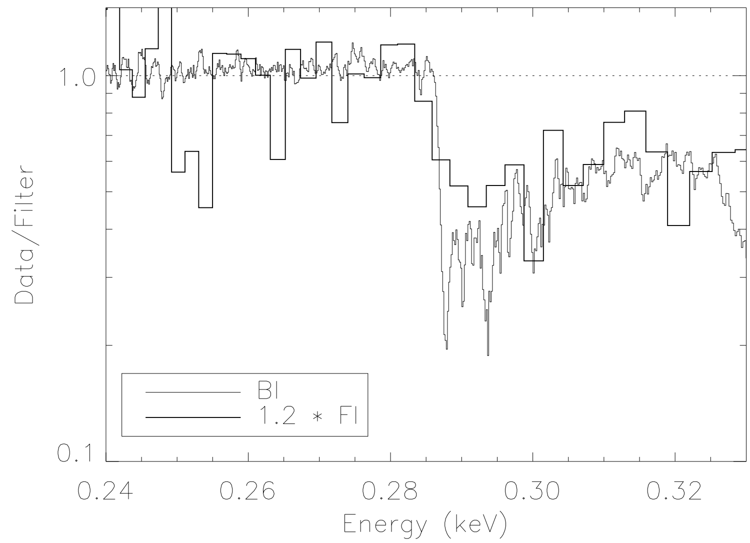

Figure 3. Data from the frontside-illuminatd (FI) chip on the +1 LETGS order are compared to the spectrum from the -1 side, which is on a backside-illuminated (BI) chip. The coarsely binned data are from the FI chip in the C-K region where the overall QE is quite low, so the data are heavily binned. Nevertheless, there is a distinct edge that is not taken into account in the OBF filter model. The FI data agree reasonably well with the BI results, after accounting for a systematic QE difference of 20%, except that the BI data are somewhat lower than the FI data near 0.29 keV.

where $x \equiv (\lambda_{C-K} - \lambda)/\lambda_{C-K}$ and λ_{C-K} is the wavelength of the edge: 43.25 Å (0.2867 keV). The constants of the adjustment were estimated (chi-by-eye): $A = 0.4$, $x_d = 4.0/\lambda_{C-K}$, and $f = 2\pi\lambda_{C-K}/16$. These provided a sharp increase in the opacity just to the high energy side of the edge which damps out to higher energies so that it is asympotically equivalent to the form from the CXRO web site. The oscillatory term accounts for the "ripple" of the deviation. The near edge X-ray absorption feature near 0.286 keV was added to the model empirically as a new shallow edge. This shallow edge was actually detected in the observation of XTE J1118+48 (Fig. 2) but was modeled by a 13% adjustment of the filter; upon increasing to an optical depth of 30%, it was clear that this feature was part of the C-K edge structure of the contaminant. Thus, the 13% filter adjustment was not applied when developing the C-K edge model upgrade. The new model of the C-K edge is folded with the instrument response and shown against the PKS 2155-304 data in Fig. 6 and clearly shows the small extra absorption in the 0.285-0.287 keV region.

3.2. Modeling the F-K and O-K Edges

As with PKS 2155-304, we extracted the observed count spectrum, n_E, for the Mk 421 observation in October 2002 (obs ID 4148, provided by F. Nicastro). This time, the C-K edge model was included with the model of N_E, allowing the depth of the edge to vary using a single depth parameter. The optical depth due to absorption is computed as before and is plotted in Fig. 7. The structure of the O-K edge is very similar to the O-K edge found in the ACIS optical blocking filter. The model was taken from a spectral decomposition of the OBF[5] and then matched to the Henke optical constants in the 18-21 Å region for extrapolation shortward of 18 Å. This model has a resonance feature that shows up as a deep narrow absorption line near 23.3 Å that is clearly detected.

The edge at 18 Å (0.69 keV) is attributed to the fluorine K edge. Fig. 7a shows that the edge cannot be identified with redshifted Fe-L. The F-K edge extended fine structure was then fit by a similar method used to fit the C-K. First, the Henke optical constants were obtained from the CXRO. Then, the edge was positioned at $\lambda_{F-K} = 18.03$ Å (0.688 keV) and fit using eq. 2 but substituting λ_{F-K} for λ_{C-K}. The constants of the adjustment were estimated: $A = 0.6$, $x_d = 4./\lambda_{F-K}$, and $f = 2\pi\lambda_{F-K}/8.5$. Note the similarity of the parameters to that

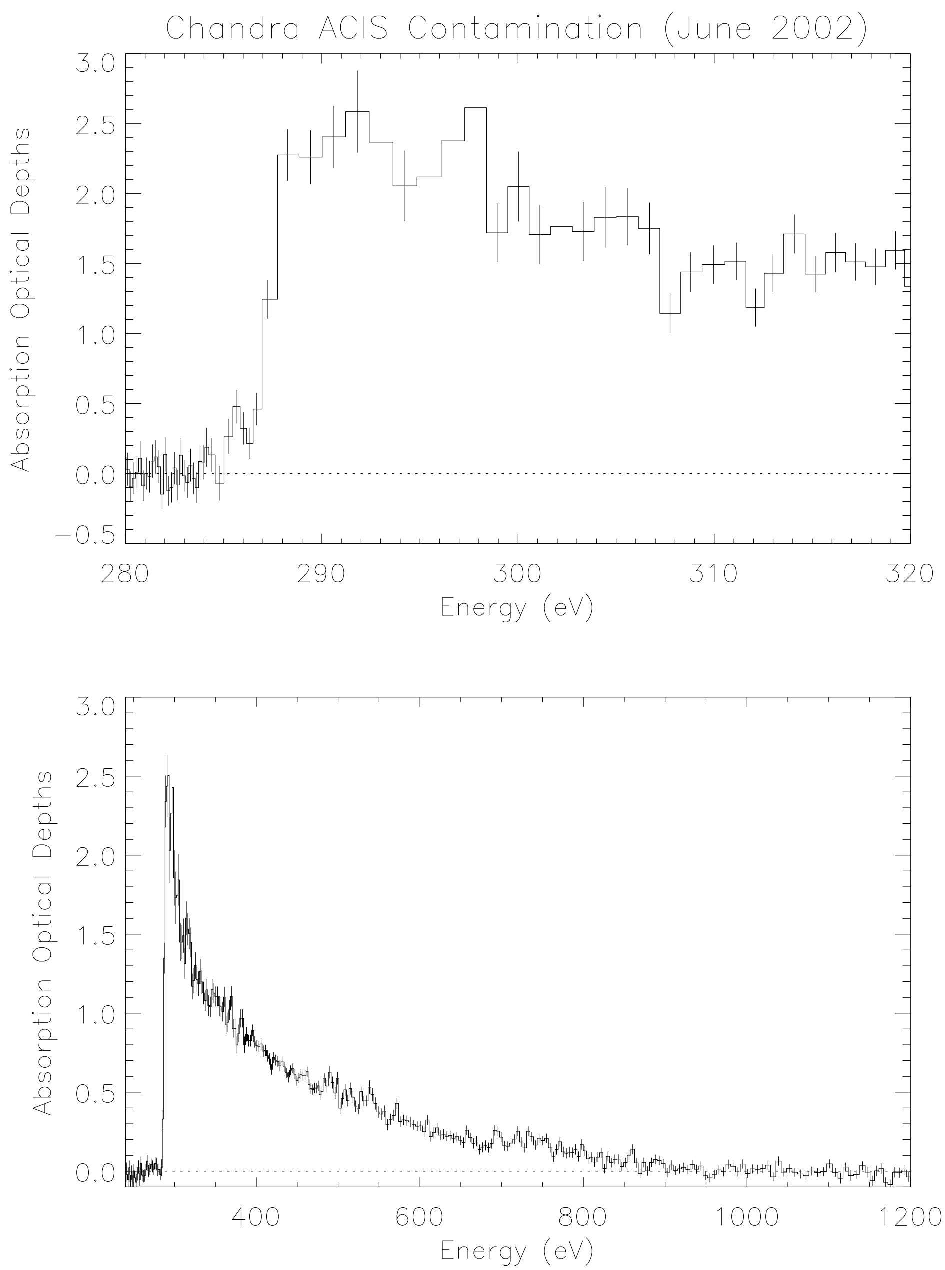

Figure 4. The optical depth of the contaminant as a function of energy, derived by adaptively binning the observed spectrum, n_E, fitting to a model, N_E, given by eq. 1 and computing $\tau(E) = -\ln(n_E/N_E)$. There are several features to notice. There is a detectable opacity beteween 0.285 keV and 0.287 keV that was not obvious previously. Above the edge at 0.287 keV, there is a monotonic decline except for some possible structure near 0.5 keV (near the O-K edge) and 0.7 keV (near the F-K edge).

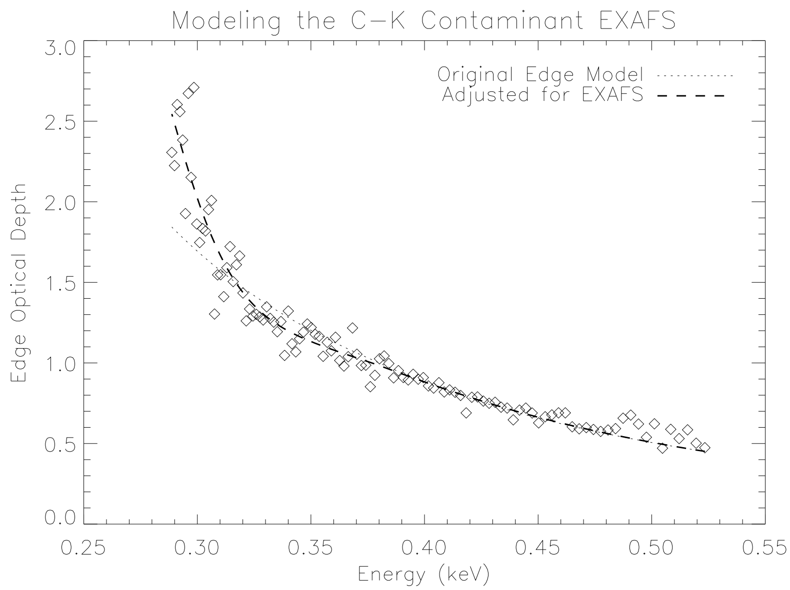

Figure 5. Similar to the bottom half of Fig. 4 except the data have been rebinned to reduce statistical noise and only the region being fit for extended fine structure is shown. The Henke model of the C-K edge (short dashed line) is a good match to the data in the 0.38 to 0.48 keV range, so the Henke optical constants are used above 0.48 keV. Below 0.38 and down to the edge, a damped oscillation adjustment is used (eq. 2).

used in fitting the C-K edge. The result is shown in Fig. 7b. The overall fit to the Mk 421 data in the 0.22-1.0 keV region is shown in Fig. 8.

3.3. Elemental Abundances

The resulting spectral model of the contaminant absorption is available in a file at the HETGS calibration web site.[†] There are four columns, corresponding to wavelength (Å) and the remaining three correspond to the absorption in optical depths due to carbon, oxygen, and fluorine. The fits gave (Henke equivalent) edge optical depths of 2.09 ± 0.02, 0.07 ± 0.03, 0.100 ± 0.007, and 0.066 ± 0.005 for the C-K, N-K, O-K and F-K edges, respectively, for the reference date of JD 2452574.0. We obtain the following column densities for C, O, and F: 2.0×10^{18}, 1.75×10^{17}, and 1.45×10^{17} atoms cm^{-2}. For N-K, the PKS 2155-304 data provided a better upper limit of the edge optical depth of about 5%, giving a column density of 7.1×10^{16} atoms cm^{-2}. Carbon is more abundant than the other elements by factors of 11.5, 14, and >30 for F, O, and N, respectively. The uncertainties on these ratios are about $\pm$ 1. Using this model, the mass surface density as of early August 2003 is 56 μg cm^{-3}. For an estimated density of 1.5 g cm^{-3}, the contaminant should be about 370 nm thick. For comparison, the thickness of the ACIS OBF is 330 nm.

4. COMPARING TO TRANSMISSIONS OF KNOWN COMPOUNDS

Detecting F-K in the absorption spectrum indicates that some portion of the contaminant is related to on-board fluorocarbon-based compounds such as Braycote 601 and Krytox, which are used in the *Chandra* mechanisms. However, the abundance ratios measured in the contaminant are not found in any of the materials actually aboard the spacecraft. The contaminant is much more carbon rich than any known fluorocarbon. Therefore, we are not detecting these compounds directly.

Another clue to the origin of the contaminant comes from the structure of the absorption near the C-K edge. In fig. 9, we compare the absorption spectrum of the ACIS contaminant near the C-K edge to those of a

[†]See `http://space.mit.edu/CXC/calib/contamination_model.txt`.

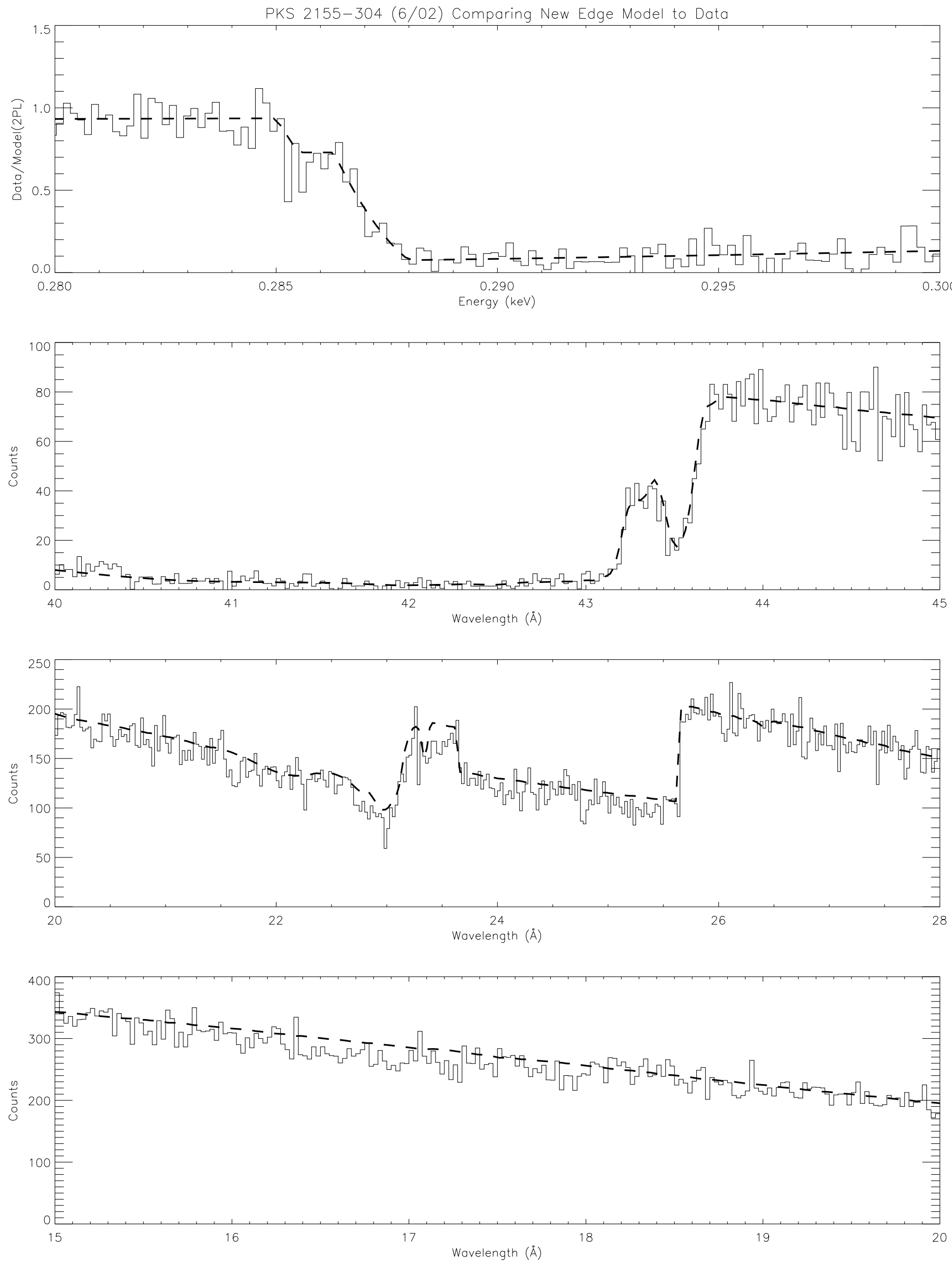

Figure 6. Comparison of the new C-K edge model with data from a long PKS 2155-304 observation. The top panel shows the ratio of the data to the model without including contamination so that the near edge structure is apparent and the new model of the absorption due to contamination is overlaid. The remaining panels show the model with the new absorption model folded with the effective area. The data fit the new model well with a slight systematic offset starting near 25.6 Å where there is a jump where one side goes from a BI chip to a FI chip, so the systematic deviation from 20 to 26 Å is primarily due to a slight error in the correction to bring the QEs of these chips into agreement. One can also begin to see the 18 Å (0.69 keV) edge due to F-K that is modeled using a bright Mk 421 observation and was ignored when fitting this C-K edge model.

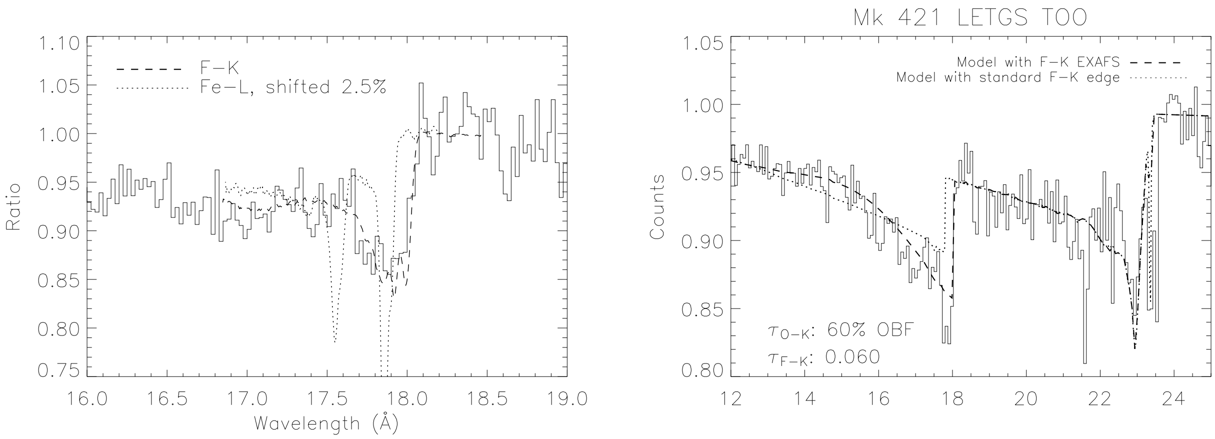

Figure 7. a) (Left) The 18 Å (0.688 keV) edge is compared to two models. The dotted line represents possible Fe-L absorption, redshifted to $z = 0.025$. The lines are too narrow to fit the data. The F-K edge, however, fits very well without shifting. F-K and Fe-L opacity data were obtained by measuring the X-ray transmission of perfluoro-adamantine and butadiene iron tricarbonyl with a scanning transmission X-ray microscope.[6] **b)** (Right) Modeling the 12-25 Å (0.5-1 keV) region of the Mk 421 X-ray spectrum. The O-K absorption is dominated by a resonance feature at 23.35 Å (0.531 keV) and a deep edge at 23.0 Å (0.540 keV). Other narrow features in this region are associated with the source or the interstellar medium. The 18 Å (0.69 keV) edge is modeled using Henke optical constants for fluorine with a modification factor given by eq. 2 and shifting the edge to 18.03 Å (0.688 keV).

number of hydrodcarbon and fluorocarbon species similar to species used in Chandra. The sharp peaks at 0.285 keV are associated with C=C double bonds present in unsaturated and aromatic molecules. Fluorocarbons like teflon, Braycote and Krytox have sharp structures in the 0.289-0.296 keV range associated with C-F bonds. The ACIS contaminant shows neither of these features. Aliphatic hydrocarbons (those containing only of mainly C-C single bonds) have a C-K edge which is broad with relatively little structure, similar to that observed for the ACIS contaminant. We conclude that the contaminant is predominantly aliphatic; i.e., consisting mostly of hydrocarbons.

We surmise that the contamination material is actually a product of radiation damage of fluorocarbon based materials. C-F bonds are readily broken by X-rays or cosmic rays leading to loss of fluorine, which flies off as FH,F_2, or a small fluorocarbon. If the radiation-damaged fluorocarbon remains on the detector or filter surface, the damage event leaves behind a carbon-rich residue, which could bind quite strongly and build up over time.

5. TIME DEPENDENCE

Using the contamination model derived above, the LETG/ACIS data were fit for many sources with smooth spectra, allowing the C-K, O-K, and F-K edges to vary independently. The results are shown in Fig. 10. Then the C-K edge depth was fit to a simple time dependence model. The data are well fit by a linear model but a perhaps more physical model was adopted to allow the optical depth to be zero at the time of the opening of the ACIS door. The equation for the time dependence is

$$\tau = a(t - y_0) - a(t_0 - y_0)e^{\frac{t-t_0}{q}}, \tag{3}$$

where τ is the C-K optical depth, a is the asymptotic rate of increase (0.455 opt. depths per year), t_0 is the date (1999.70) at which τ is forced to be zero, y_0 is the year (1998.32) at which the linear regression gives $\tau = 0$, and q is the estimated timescale on which the optical depth approaches the asymptotic form: 0.15 yr.

The shape of the time dependence was assumed to be the same for each of the three detected edges and were merely scaled to observed optical depths (see the previous section) for the date of the Mk 421 observation (year

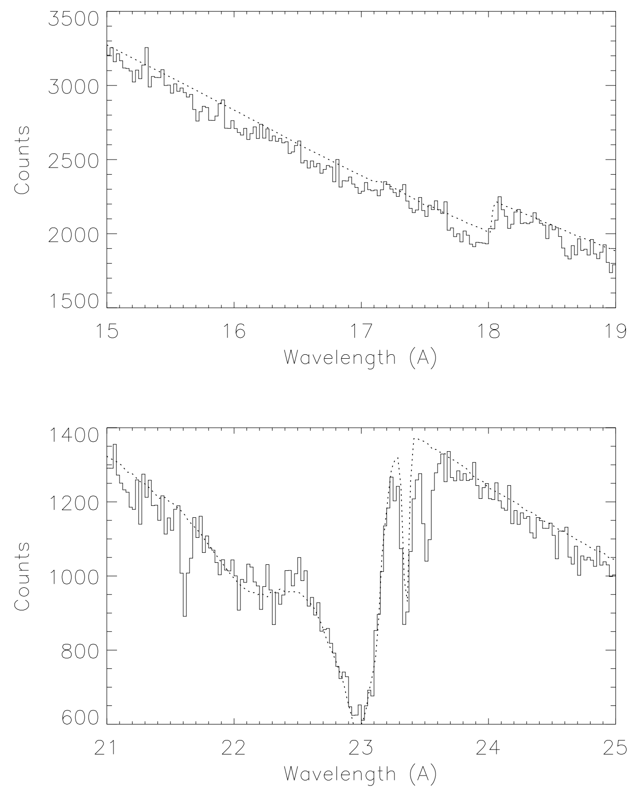

Figure 8. Count spectra at the edges of F-K (top) and O-K (bottom). The overall structure is modeled to better than 3% and the only remaining features are intrinsic to the source (or to the gas between the target and the telescope, see Nicastro et al. 2003, in preparation). There is a slight normalization error in the F-K edge region due to the systematic effects of correcting for the relative error in the BI QEs compared to the FI QEs.[4]

2002.86). Because the optical depth values used to create the contamination model were slightly different – 2.10, 0.09, and 0.06 (for C-K, O-K, and F-K, respectively) – the time factors for each component were merely rescaled. The resulting time dependence file is available on-line.[‡]

The O-K edge data do not fit the model as well as expected for reasons that are not completely understood. Fig. 10 shows that the O-K edge measurements are mostly below the model. These deviations are not readily explained by O-K in the interstellar medium (ISM). In all the PKS 2155 measurements, for example, the N_H was free and varied between 1.0 and 1.7×10^{20} cm^{-2}. The "nominal" value is about 1.35×10^{20} cm^{-2}, for which two different ISM models give an O-K edge of 0.054 optical depths. If the N_H were systematically decreased to 1.0×10^{20} cm^{-2}, say, then the average O-K due to the contaminant would increase by 0.027 – which is insufficient to explain the difference between the model and the data.

6. COMPARISON TO THE EXTERNAL CALIBRATION SOURCE

Plucinsky *et al.*[1] showed how the ratio of the L line fluxes in the External Calibration Source (ECS) relative to the Mn K line flux is a monotonically decreasing function of time. This flux ratio appears to be a direct measure of the transmission of the contaminant at the energies of the lines in the L line complex. Several lines are expected, dominated by the α_1 and α_2 lines of Fe and Mn at 705.0 and 637.4 eV, respectively. The F-K edge falls between these energies and it is a fortuitous circumstance that the transmission through the contamination

[‡]See `http://space.mit.edu/CXC/calib/time_factor.txt`.

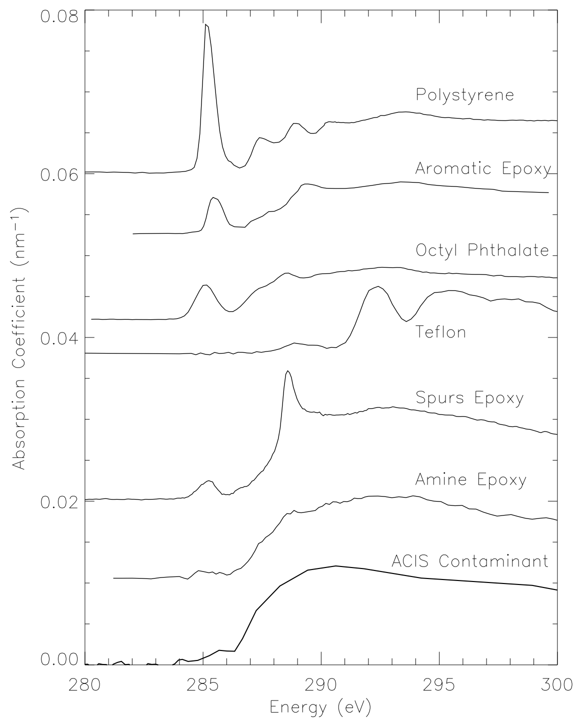

Figure 9. Comparison of the opacity of the ACIS contaminant near the C-K edge to those for 6 different materials measured using a scanning transmission X-ray microscope.[6] The intensity scales of the reference opacities are quantitative linear absorption per nm of material; that for the contaminant has been scaled to have a similar amplitude. Arbitrary offsets are used for clarity. The absorption spectra of compounds containing C=C or C=O double bonds or C-F single bonds do not match the spectra of the contaminant. A good match is found to an aliphatic amine epoxy.

absorption model developed here is very nearly the same at these two energies, so we choose $E = 700$ eV at which to evaluate the absorption model for comparison to the ECS data, shown in Fig. 11. The L/K ratios have been converted to optical depths for ease of comparison with the contamination model.

Fig. 11 shows that the contamination model developed here explains about 80% of the opacity that absorbs the ECS L lines. We cannot as yet explain what causes the remaining 20%, which is 0.1 optical depths at the present time (mid-2003). Thus, using this contamination model may result in systematically low fluxes by 10% in observations if the ECS gives an accurate portrayal of the absorption on the detector focal plane. Due to the relatively high temperature expected for the ECS, it seems unlikely that sufficient contaminant has condensed on the ECS itself that might explain this difference. One possibility is that the radiation-generated molecular fragments have a range of sizes that would result in a range of condensation temperatures, so that the ECS-LETGS differences might provide an estimate of the fraction of fragments with high condensation temperatures.

One class of attempts to explain the extra 0.1 optical depth at 700 eV involve adding some other material in the contaminant but most of these would have clear spectral edges at higher energies (in the case of Si and Mg). Hydrogen wouldn't show an edge in the LETGS band but the column density that would be required to give an optical depth of 0.1 at 700 eV is 2.7×10^{21} cm^{-2}, or 1300 atoms of H per atom of C. It would seem to be an unlikely mixture that would somehow adhere to the ACIS detector. One interesting possibility is Au, used as a coating in much of ACIS. It would require only a 50 nm layer to provide an opacity of 10% at 700 eV and yet the M edge at 2.3 keV would have a depth of only 2%. Such an edge is difficult to measure at present, given the strong edge due to Au in the gratings themselves.

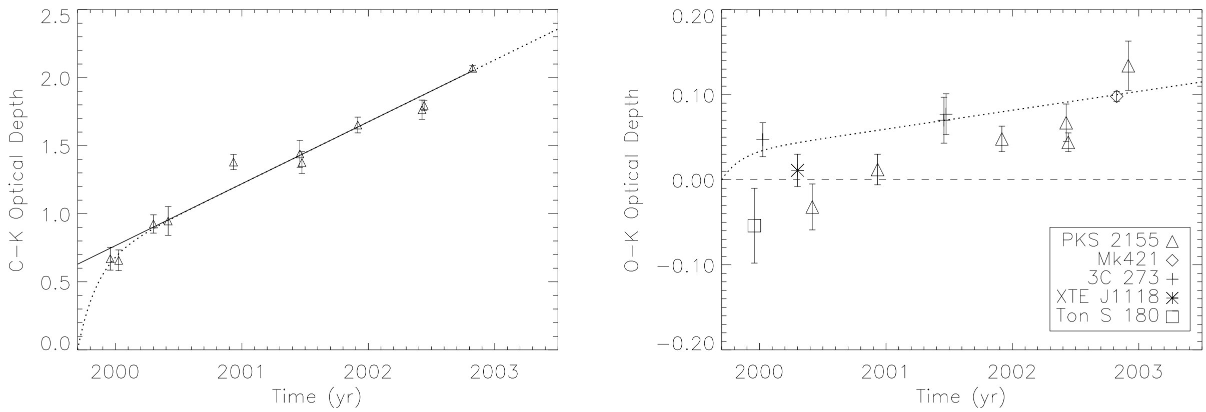

Figure 10. a) (Left) The C-K edge optical depth as a function of time for 11 observations of essentially featureless sources observed with the LETG and ACIS. The solid line is a linear regression that is not forced to go through zero, while the dashed line is a model with similar asymptotic behavior that is forced to zero at ACIS door opening. **b)** (Right) O-K edge measurements as a function of year compared to the model for the time dependence of the O-K optical depth. The model assumes that the O-K optical depth scales with the C-K edge and is forced to go through the best data point (Mk 421, in late 2002). In general, the trend given by the model is matched by the data: the O-K edge is detected only in the last year or so and is smaller in the first year. In particular, the possibility that the O-K edge is nearly constant after 2000.0 seems to be ruled out.

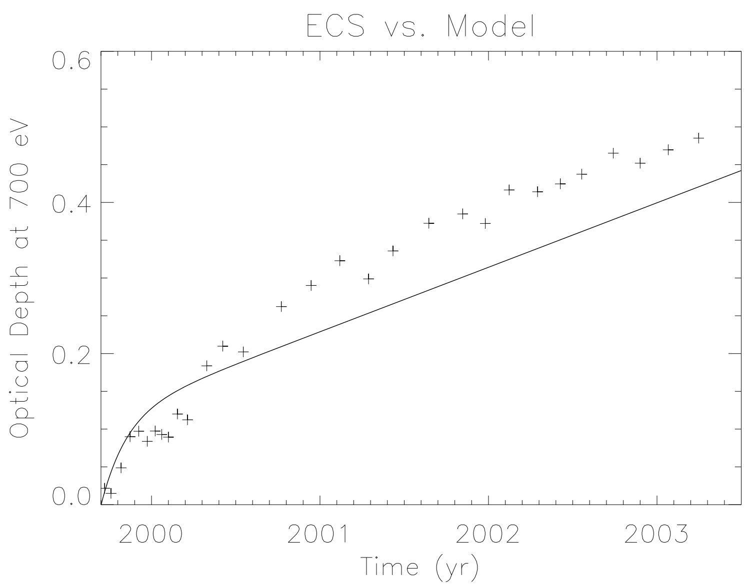

Figure 11. The optical depth at 0.70 keV determined from the ratio of the fluxes in the external cal source (ECS) Mn L and Fe L lines to the flux of the Mn K line integrated over the entire S3 (BI) chip as a function of time for the first 3.5 years of *Chandra* operations. Also shown is the model of the time dependence derived from fits to the C-K edges (see fig. 10). The contamination model is 20% lower than the computed optical depth over the last two years. The difference is about 0.1 optical depths, corresponding to a 10% difference in total transmission.

7. FURTHER WORK

We have obtained X-ray transmission data for a sample of Braycote and found that the material was quite sensitive to irradiation. We are preparing results on the x-ray transmission of the radiation-damaged oil. Preliminary results indicate that the X-ray transmission changes character in the manner expected: the 0.289 keV opacity maximum shifts downward to 0.287 keV, where it is found in the *Chandra* system. We will also test for changes at the F-K edge.

We have recent evidence that the contaminant opacity varies somewhat from center to edge. Although spatial nonuniformity affects the comparison of the ECS and LETGS results, the discrepancy between these estimates of the opacity at 0.7 keV (fig. 11) remains unexplained.

ACKNOWLEDGMENTS

This work was supported in part by contracts SAO SV1-61010 and NAS8-39703. We thank Dan Dewey for useful comments on the manuscript.

REFERENCES

1. P. P. Plucinsky, N. S. Schulz, H. L. Marshall, C. E. Grant, G. Chartas, D. Sanwal, M. Teter, A. A. Vikhlinin, R. J. Edgar, M. W. Wise, G. E. Allen, S. N. Virani, J. M. DePasquale, and M. T. Raley, "Flight spectral response of the ACIS instrument," in *X-Ray and Gamma-Ray Telescopes and Instruments for Astronomy. Edited by Joachim E. Truemper, Harvey D. Tananbaum. Proceedings of the SPIE, Volume 4851, pp. 89-100 (2003).*, pp. 89–100, Mar. 2003.
2. M. C. Weisskopf, B. Brinkman, C. Canizares, G. Garmire, S. Murray, and L. P. Van Speybroeck, "An Overview of the Performance and Scientific Results from the Chandra X-Ray Observatory," *PASP* **114**, pp. 1–24, Jan. 2002.
3. G. P. Garmire, M. W. Bautz, P. G. Ford, J. A. Nousek, and G. R. Ricker, "Advanced CCD imaging spectrometer (ACIS) instrument on the Chandra X-ray Observatory," in *X-Ray and Gamma-Ray Telescopes and Instruments for Astronomy. Edited by Joachim E. Truemper, Harvey D. Tananbaum. Proceedings of the SPIE, Volume 4851, pp. 28-44 (2003).*, pp. 28–44, Mar. 2003.
4. H. L. Marshall, D. Dewey, and K. Ishibashi, "In-flight calibration of the Chandra high-energy transmission grating spectrometer," in *X-Ray and Gamma-Ray Telescopes and Instruments for Astronomy. Edited by Kathryn A. Flanagan, Oswald H. W. Siegmund. Proceedings of the SPIE, Volume 5165, these proceedings.*, 2003.
5. G. Chartas, G. P. Garmire, J. A. Nousek, L. K. Townsley, F. R. Powell, R. L. Blake, and D. E. Graessle, "ACIS UV/optical blocking filter calibration at the National Synchrotron Light Source," in *Proc. SPIE Vol. 2805, p. 44-54, Multilayer and Grazing Incidence X-Ray/EUV Optics III, Richard B. Hoover; Arthur B. Walker; Eds.*, pp. 44–54, July 1996.
6. A. L. D. Kilcoyne, T. Tyliszczak, W. F. Steele, S. Fakra, P. Hitchcock, K. Franck, E. Anderson, B. Harteneck, E. G. Rightor, G. E. Mitchell, A. P. Hitchcock, L. Yang, T. Warwick, and H. Ade, "Interferometrically controlled scanning transmission microscopes at the advanced light source," *J. Synchrotron Radiation* **10**, pp. 125–136, 2003.